



Impact of laser flicker noise and linewidth on 64 to 96 Gbaud/DP-nQAM metro coherent optical links

RUI ZHANG,^{1,*} KONSTANTIN KUZMIN,² WEN-JR JIANG,² GIORGIO GIARETTA,² TADATOSHI TOMIMOTO,² YI WENG,² GEE-KUNG CHANG,¹ AND WINSTON WAY²

¹School of Electrical and Computer Engineering, Georgia Institute of Technology, Atlanta, Georgia 30332, USA

²NeoPhotonics, 3081 Zanker Road, San Jose, California 95134, USA

*Corresponding author: ruizhangce@gatech.edu

Received 6 January 2020; revised 20 January 2020; accepted 21 January 2020; posted 22 January 2020 (Doc. ID 386267); published 26 February 2020

We experimentally investigate the impact of laser flicker noise and linewidth on 64 Gbaud/DP-64QAM, 96 Gbaud/DP-32QAM and 64 or 96 Gbaud/DP-16QAM links. To give a more practical viewpoint, the examined flicker noise closely follows that of an industry forum (OIF 400ZR). We have found that higher modulation order (e.g., 64QAM) is sensitive to phase noise from the linewidth and flicker noise, even in the back to back case. Significant optical signal to noise ratio (OSNR) and cycle slip rate penalties can also be observed with a transmission distance >200 km for both 64QAM and 32QAM signals, which mainly comes from equalization-enhanced phase noise. Moreover, with the increasing of transmission distances, the effective linewidth of a tunable laser with a higher flicker noise and higher linewidth (210 KHz) increases significantly, while it remains unchanged for an external cavity laser (ECL) with 47-kHz linewidth. The result indicates the importance of more stringent flicker noise and linewidth requirement for future ultrabaud rate transmissions. © 2020 Optical Society of America

<https://doi.org/10.1364/OL.386267>

It has been shown that the coherent system penalty due to equalizer-enhanced phase noise (EEPN) is mainly caused by fiber chromatic dispersion and the frequency noise of a local oscillator (LO) [1]. The frequency noise includes flicker noise [2] and interfering tones [3] below 1–100 MHz, and white (Wiener) frequency noise between ~10 MHz and ~1 GHz in a state-of-the-art semiconductor tunable laser. The white frequency noise power spectral density (PSD) is directly related to a laser's Lorentzian 3 dB linewidth $\Delta\nu$ by a factor of π , while $\Delta\nu$ affects error vector magnitude (EVM) for all orders of QAM modulations through $EVM^2 \propto [\Delta\nu \times B_s \times L]$, where B_s is the baud rate, and L is the fiber transmission length [1]. A sinusoidal interfering tone affects signal EVM through $EVM^2 \propto [\Delta f_{pp} \times B_s \times L]^2$ above a corner frequency of

~1 MHz, where Δf_{pp} is the laser peak-to-peak frequency deviation due to the sinusoidal tone [3].

Flicker noise in a distributed Bragg reflector (DBR) tunable laser, on the other hand, has been shown to cause significant coherent system penalty even without any transmission fiber [2,4]. However, the examined flicker noise level was excessively high due to the current injection-induced carrier density fluctuation in the phase sections. This excessive frequency noise can be reduced by using thermal tuning instead [5]. In our experimental study, we have used a thermally-tuned DBR LO whose flicker noise PSD closely follows that of an industry forum (OIF 400ZR).

In this Letter, through experimental analysis with a phase modulator, we have found that, for a higher order QAM such as 64QAM, the flicker and Wiener frequency noise cause an appreciable optical signal to noise ratio (OSNR) penalty even without fiber transmission. Moreover, the flicker noise above 1 MHz in the frequency noise PSD also causes significant EEPN-induced OSNR and cycle slip rate penalties in a 96 Gbaud/DP-32QAM system when the transmission distance is beyond 200 km. Compared with a back to back (BtB) case, the phase fluctuations from the flicker noise and higher linewidth will be more significant in the case of 450-km transmission, while that of the external cavity laser (ECL) remains unchanged.

The experimental setup is shown in Fig. 1. The transmitter is a 193.5 THz ECL, and three types of LOs were used: an ECL ($[\Delta\nu = 47 \text{ kHz}]$), a DBR ($[\Delta\nu = 210 \text{ KHz}]$), and the same DBR with additional injected flicker noise to make its frequency noise match with that of the OIF 400ZR mask. The latter was achieved by using a phase modulator (PM) and a low-speed arbitrary waveform generator (AWG) to modulate the phase of the DBR LO. The frequency noise (FN) PSD for the DBR (PSD A) and DBR with additional flicker noise (PSD B) are shown in the Fig. 2. We see that PSD B has additional flicker noise between 1 and 70 MHz, which matches with the OIF mask very well. For the area between 70 and 100 MHz, PSD B falls slightly below the OIF Mask due to bandwidth limitation of the PM.

At the transmitter side, four uncorrelated data sequences were loaded to an InP coherent driver modulator (CDM)

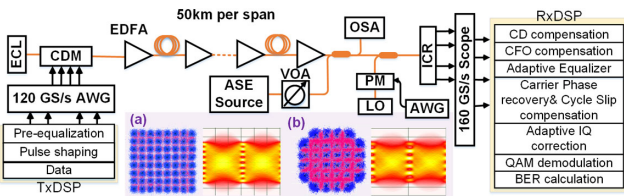


Fig. 1. Experimental setup of the 64/96-Gbaud optical coherent systems. EDFA: erbium-doped fiber amplifier, OSA: optical spectrum analyzer. Insets (a) and (b): constellations and eye diagrams of the recovered 64-Gbaud/DP-64QAM and 96-Gbaud/DP-32QAM signals, respectively, for one of the polarizations. Red points correspond to erroneous symbols; blue points are symbols without errors.

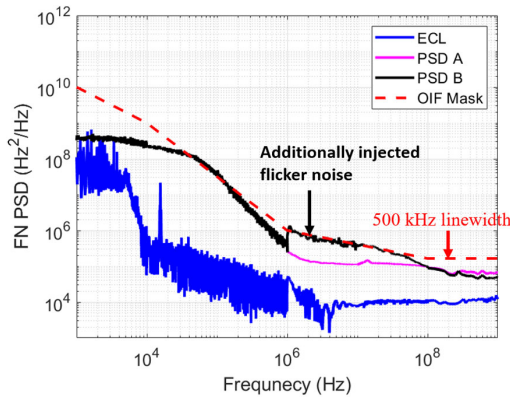


Fig. 2. Frequency noise (FN) PSD of a ECL, a DBR laser (PSD A), and a DBR with additional flicker noise injected from a phase modulator (PSD B) to match the 400ZR OIF mask.

through a 120 G/s AWG whose 6 dB bandwidth is 47 GHz. The peak-to-peak driving voltage is $0.7 \text{ V}\pi$. The 6-dB bandwidth of the CDM is 49 GHz (including the effect of an evaluation board and cables). Pulse shaping with a roll-off factor of 0.2 was employed. Pre-equalization via 100 taps was utilized to compensate for the bandwidth limitation at the transmitter side. The maximum transmission distances for 64 Gbaud/DP-64QAM and 96 Gbaud/DP-32QAM were 450 km (with a chromatic dispersion (CD) emulator having an insertion loss of 8 dB) and 400 km (with a span length of 50 km), respectively. Note that a CD emulator cannot be used for the 96-Gbaud system due to its limited 3-dB optical bandwidth of 64 GHz. The input power for each fiber span is set at 0 dBm/channel. At the receiver side, an InP intradyne coherent receiver (ICR) with a 6-dB bandwidth of 51 GHz (including the effect of an evaluation board and cables), and a 160-GS/s scope and an off-line DSP were used. The input signal and LO power to the ICR were -6 dBm and $+12.5 \text{ dBm}$, respectively. In the receiver DSP, the signal was resampled to two samples per symbol, followed by a CD and a constant frequency offset (CFO) estimation and compensation. A 4×2 butterfly adaptive equalizer is then employed to perform polarization demultiplexing, and additional compensation of fiber PMD, residual CD, and residual clock frequency error. The adaptive equalizer (AE) uses a training sequence for preconvergence and LMS for tracking. Because the AE is implemented in the frequency domain, the taps and carrier phase are updated with a time interval equals to $n\text{Taps}/(2B_s)$. After the AE, the blind phase search (BPS) [6] algorithm with 64 test

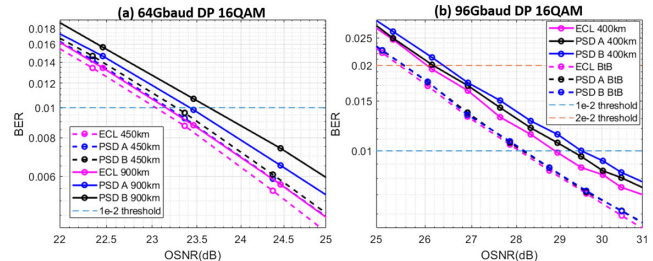


Fig. 3. BER versus OSNR in (a) 64 Gbaud DP 16-QAM transmission and (b) 96 Gbaud DP 16-QAM transmission.

angles and 65 symbols sliding window averaging is used to refine the carrier phase estimation. Note that the BPS algorithm gives a better OSNR performance than a pilot-aided phase recovery algorithm [7,8], e.g., 1 in 32 pilot injection in OIF 400ZR Implementation Agreement. The phase noise-induced OSNR penalty would be higher than what we report here if a pilot-aided algorithm is used. After the carrier phase recovery, an adaptive IQ correction [9] is used to compensate for Tx and residual Rx impairments. Finally, demodulation and BER counting were performed.

First, we investigate the FN PSD impact on 64 Gbaud or 96 Gbaud DP 16-QAM signal. Figure 3 presents the experimental results. The tap numbers for all types of LOs are 64. For back to back (BtB) transmission, there is no OSNR penalty for different LOs. However, EEPN becomes more stringent with the increasing of fiber distances. In Fig. 3(a), we can observe that, different types of LOs induce little OSNR degradation (~ 0.1 to 0.2 dB) in 64 Gbaud 450-km transmission. However, in case of a 900-km transmission, compared with ECL, PSD A shows 0.3-dB OSNR degradation at the BER of $1e-2$ while PSD B shows 0.5-dB penalty. For higher baud rate (96 Gbaud) as shown in Fig. 3(b), compared with ECL at the BER of $1e-2$, PSD B induces 0.5-dB OSNR penalty, while PSD A shows 0.3-dB OSNR penalty with a 400-km fiber dispersion.

Different from 16QAM signals with the same AE tap number for different types of LOs, the 64-Gbaud/DP-64QAM signal is very sensitive to LO phase noise. Therefore, different AE tap numbers were used for different types of LOs to optimize the system performances. A larger AE tap number such as 64 has more symbols in a processing block, so more AWGN can be removed due to additional averaging. However, a higher order of modulation is more sensitive to phase fluctuations and consequently requires a smaller tap number and processing block to better track the phase variation. In our experiment, for the LO with a frequency noise PSD A and PSD B, the BER performances become unstable when we employ larger tap number (e.g., 64), especially in case of lower OSNR. Therefore, the optimized tap numbers were 64, 32, and 16 for the ECL LO, the LO with FN PSD A and B, respectively, which indicate the different levels of phase noise fluctuation for the three cases. Figure 4(a) shows that for 64 Gbaud/DP-64QAM, a significant OSNR performance difference exists among the three types of LO even in the BtB condition. In comparison to an ECL, the LO with PSD A incurred 0.4-dB OSNR penalty at a BER of $3.77e-2$ (which corresponds to an FEC overhead of 25.5% and net coding gain of 12 dB [10]), while the LO with PSD B incurred a penalty of 1 dB. An FEC with a smaller overhead would cause higher OSNR penalties. For example, PSD A and

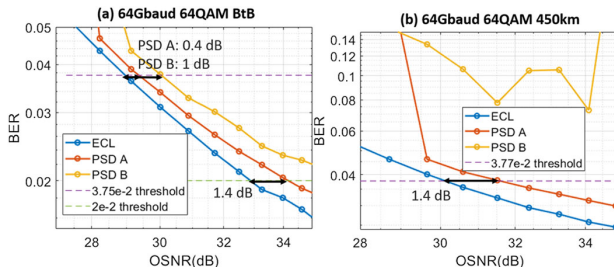


Fig. 4. BER versus OSNR in (a) 64 Gbaud DP 64-QAM BtB transmission and (b) 64 Gbaud DP 64-QAM 450-km transmission.

B incurred 1.4-dB and $\gg 2$ -dB OSNR penalty at a BER of $2e-2$, respectively. The penalties mainly come from different tap numbers, hence different levels of AWGN removing.

Next, the EEPN effect was investigated by using a 450-km CD emulator, and the results are shown in Fig. 4(b). The LO with a frequency noise PSD B fails with 450-km fiber dispersion, while the LO with a frequency noise PSD A incurred a 1.4-dB OSNR penalty at a BER of $3.77e-2$.

It is worthwhile to compare the phase fluctuations of the three types of LOs at the adaptive equalizer with and without fiber transmission. Figure 5 presents the estimated phase fluctuation over time in different LOs at an OSNR of 35 dB in the 64 G/DP-64QAM experiment. The effective laser linewidth can be obtained from Fig. 5 via the phase difference variance through

$$LW_{\text{eff}} = \frac{\text{var} \langle \Delta\phi \rangle}{2\pi\tau}, \quad (1)$$

where $\text{var} \langle \Delta\phi \rangle$ denotes the phase difference variance, and τ is the time interval between two phases. For a fair comparison, we used the same time interval ($\tau = 64/(2 \cdot B_s)$) to calculate the effective linewidth for all laser types. Note that the effective linewidth is a good reference for comparison of phase variations caused by different lasers. We observe that, in both BtB and after 450 km CD emulator, ECL exhibits smooth curves, while PSD A and B exhibit significant phase fluctuations. The ECL effective linewidths before and after the 450 km SMF are the same, and match well with the actual measurement. For PSD A, after the 450 km CD emulator, the effective linewidth increases from 192.7 kHz (which matches well with measurement) to 329.3 kHz. The introduction of extra frequency flicker noise in PSD B causes the effective linewidth to change significantly from 458.8 kHz (which is much higher than the measured 210 KHz linewidth, due to the additional flicker noise) to 610 kHz after 450 km CD emulator. Note that in a real-time system, the symbol rate and ADC sampling frequency are higher than the DSP clock frequency, thus the carrier phase recovery algorithm needs to resort to parallel processing or a pilot-aided algorithm [7], which in turn makes the phase noise tolerance significantly reduced compared to our results presented here [11].

In the 96-Gbaud/DP-32QAM transmission experiment, the signal is found to be less sensitive to phase variation than the 64-Gbaud/DP-64QAM signal. Hence, the same as the 16QAM signal, all three types of LO share the same AE tap number of 64. Also, in a BtB setup, the BER versus OSNR performance becomes very close for all three types of LO. However, the EEPN-induced OSNR penalty increases with the transmission

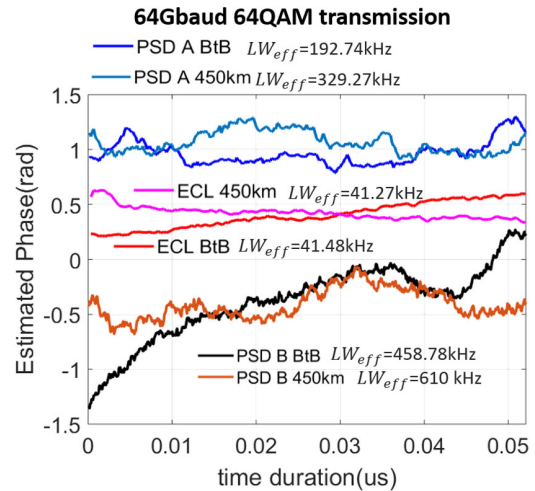


Fig. 5. Estimated phase fluctuations versus time duration in 64-Gbaud/DP-64QAM BtB and 450-km transmission.

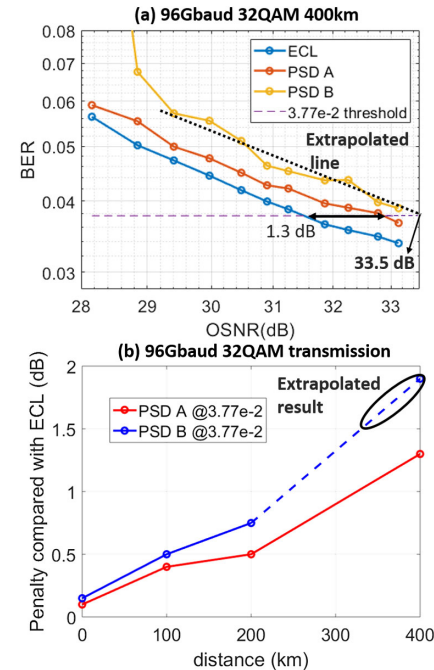


Fig. 6. (a) BER versus OSNR for 96-Gbaud/DP-32QAM in 400-km fiber transmission; (b) OSNR penalty versus distance due to a DBR with PSD A or PSD B when compared with that of the ECL.

distance. As shown in Fig. 6(a), with 400-km SMF transmission, 1.3- and 1.9-dB OSNR penalties are observed when using PSD A and PSD B, respectively, at a pre-FEC BER threshold of $3.77e-2$. Note that the penalty of PSD B is an extrapolated result due to our system OSNR limit. Figure 6(b) summarizes the OSNR penalties caused by the DBR LO (with a PSD A or B) when compared to the ECL at different SMF transmission distances. For a SMF transmission under 100 km, both types of DBR exhibit ≤ 0.5 dB OSNR penalty.

However, this penalty increases with transmission distance due to EEPN, and the penalty due to the DBR LO with PSD B increases much faster than that of the DBR LO with a PSD A.

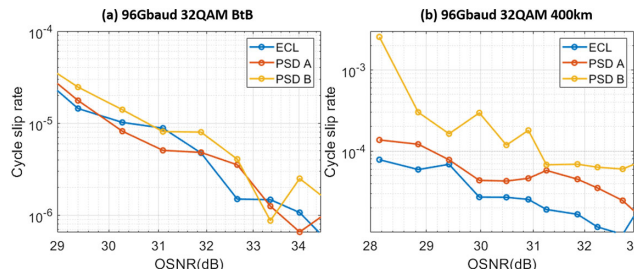


Fig. 7. Cycle slip rate versus OSNR in (a) 96 Gbaud DP 32-QAM BtB transmission and (b) 96 Gbaud DP 32-QAM 400-km transmission.

This is because PSD B has the extra flicker noise between 1 and 70 MHz in comparison to PSD A [see Figs. 2(a) and 2(b)], and these extra flicker noises can be considered as being composed of multiple uncorrelated sinusoidal tones. We have shown in Ref. [3] that the OSNR tolerance to sinusoidal tones above a corner frequency of 1 MHz is much tighter than those below the corner frequency, which is dependent on the symbol length of the CFO estimation block.

Moreover, we further investigate the cycle clip rate performance in 96 Gbaud 32-QAM systems. Different from the significant cycle slip observed in Ref. [2] for the BtB case, with additional flicker noise and higher linewidth, the cycle clip rates of PSD A and PSD B are still similar to that of ECL as shown in Fig. 7(a). With the fiber distance increases to 400 km, the cycle slip rate of PSD B increases more significantly than PSD A and ECL. The additional flicker noise or higher linewidth would induce more cycle slips with the increasing of fiber distance. This is consistent with our observations in Fig. 5.

In summary, by using a CDM and ICR evaluation boards with 6-dB bandwidths of 47 and 51 GHz, respectively, and based on an OIF 400ZR laser frequency noise mask, we have investigated the impact of laser linewidth and flicker noise on coherent systems with different QAM orders, baud rates, and transmission distances using a 25.5% FEC overhead. We have found that, despite the 16-QAM system is less affected by phase fluctuations and EEPN, the 64-QAM system is sensitive to laser linewidth and flicker noise even in a BtB case. Furthermore, the flicker noise above 1 MHz, despite its low amplitude, forbids the 450 km system to work. The 96 Gbaud DP 32-QAM system is sensitive to laser linewidth and flicker noise only beyond 200 km, and the OSNR penalty of using a DBR laser in comparing to the case of an ECL laser was up

to 1.9 dB at 400 km. Note that in practice, a real-time DSP most likely would use a simplified carrier recovery algorithm (for lower power consumption) such as pilot symbol-assisted algorithm, which cannot achieve the superior performance of BPS carrier recovery, and therefore a higher OSNR penalty than what we have observed would be incurred. The EEPN penalty is also found to be independent of the roll-off factor of pulse shaping [1]. Consequently, for future metro optical systems which transport beyond $600 \text{ G}/\lambda$, a tighter flicker noise and linewidth mask than what is currently defined in OIF 400ZR is needed for both transmitter and LO.

Funding. I/UCRC Center of Fiber Wireless Integration and Networking (FiWIN) (1539976).

Disclosures. The authors declare no conflicts of interest.

REFERENCES

1. A. Kakkar, J. R. Navarro, R. Schatz, H. Louchet, X. Pang, O. Ozolins, G. Jacobsen, and S. Popov, *J. Lightwave Technol.* **33**, 4834 (2015).
2. T. N. Huynh and L. P. Barry, in *Optical Fiber Communication Conference* (2014), paper W4K.5.
3. R. Zhang, W. Jiang, K. Kuzmin, Y. Weng, W. Mou, G. Chang, and W. I. Way, “The impact of local oscillator frequency jitter and laser linewidth to ultra high baud rate coherent systems,” *J. Lightwave Technol.* (to be published).
4. T. N. Huynh, A. T. Nguyen, W.-C. Ng, L. Nguyen, L. A. Rusch, and L. P. Barry, *J. Lightwave Technol.* **32**, 1973 (2014).
5. H. Yagi, T. Kaneko, N. Kono, Y. Yoneda, K. Uesaka, M. Ekawa, M. Takechi, and H. Shoji, *IEEE J. Sel. Top. Quantum Electron.* **24**, 6100411 (2018).
6. T. Pfau, S. Hoffmann, and R. Noé, *J. Lightwave Technol.* **27**, 989 (2009).
7. E. Börjeson, C. Fougstedt, and P. Larsson-Edefors, in *Optical Fiber Communication Conference* (2019), paper W3H.7.
8. Q. Zhuge, M. Morsy-Osman, X. Xu, M. E. Mousa-Pasandi, M. Chagnon, Z. A. El-Sahn, and D. V. Plant, *Opt. Express* **20**, 19599 (2012).
9. C. R. S. Fludger and T. Kupfer, “Transmitter impairment mitigation and monitoring for high baud-rate, high order modulation systems,” in *42nd European Conference on Optical Communication*, Dusseldorf, Germany (2016), pp. 1–3.
10. K. Sugihara, Y. Miyata, T. Sugihara, K. Kubo, H. Yoshida, W. Matsumoto, and T. Mizouchi, in *Optical Fiber Communication Conference/National Fiber Optic Engineers Conference* (2013), paper OM2B.4.
11. T. Pfau, in *Optical Fiber Communication Conference* (2014), paper W4K.1.